May the force be with you: the role of hyper-mechanostability of the bone sialoprotein binding protein during early stages of *Staphylococci* infections.

Priscila S. F. C. Gomes [1], **Meredith Forrester** [1], **Margaret Pace** [1], **Diego E. B. Gomes** [1] **and Rafael C. Bernardi** [1,*]

[1] *Department of Physics, College of Sciences and Mathematics, Auburn University, Auburn, AL, 36849*

Correspondence*:
Rafael C. Bernardi
rcbernardi@auburn.edu

ABSTRACT

The bone sialoprotein-binding protein (Bbp) is a mechanoactive MSCRAMM protein expressed on the surface of *Staphylococcus aureus* that mediates adherence of the bacterium to fibrinogen-α (Fgα), a component of the bone and dentine extracellular matrix of the host cell. Mechanoactive proteins like Bbp have key roles in several physiological and pathological processes. Particularly, the Bbp:Fgα interaction is important in the formation of biofilms, an important virulence factor of pathogenic bacteria. Here, we investigated the mechanostability of the Bbp:Fgα complex using *in silico* single-molecule force spectroscopy (SMFS), in an approach that combines results from all-atom and coarse-grained steered molecular dynamics (SMD) simulations. Our results show that Bbp is the most mechanostable MSCRAMM investigated thus far, reaching rupture forces beyond the 2 nN range in typical experimental SMFS pulling rates. Our results show that high force-loads, which are common during initial stages of bacterial infection, stabilize the interconnection between the protein's amino acids, making the protein more "rigid". Our data offer new insights that are crucial on the development of novel anti-adhesion strategies.

Keywords: mechanobiology, *Staphylococcus* infection, biofilm, adhesins, molecular dynamics

1 INTRODUCTION

Staphylococcus aureus infections have a high clinical and communal impact with an estimated mortality rate that can reach 30.2% Bai et al. (2022). The persistence of these infections lies on the *S. aureus*' ability to form biofilms Costerton et al. (1999); Archer et al. (2011); Suresh et al. (2019), and the eventual dissemination of these pathogenic bacteria throughout the body Kwiecinski and Horswill (2020). Despite the increase in sterilization and hygienic measures, modern medical devices play a key role in the transfer of these bacterial colonies through device-associated biofilm infections Wertheim et al. (2004); Otto (2009); Lister and Horswill (2014). The contamination of patients during medical and dental procedures is of increasing relevance, particularly with the emergence of drug-resistant bacteria. In the dental field, it has been estimated that the carrier prevalence of *S. aureus* in healthy adults varies from 24% to 84% Donkor and Kotey (2020). Additionally, the oral cavity is a source for cross infection and dissemination

of the infection directly into the bloodstream, increasing the likelihood of septicemia and possibly death McCormack et al. (2015); Garbacz et al. (2021); Jevon et al. (2021).

Biofilms shelter the bacteria and enhance the persistence of infection by eluding innate and adaptive host defenses González et al. (2018); Versey et al. (2021). Biofilms also form a barrier, protecting colonies from biocides and antibiotic chemotherapies Sharma et al. (2019). Adhesins play critical roles during infection, especially during the early step of adhesion when bacterial cells are exposed to mechanical stress Latasa et al. (2006). Adhesins bind to their target ligands, holding it tight to them even at extreme force loadings that largely outperform classical binding forces Gomes et al. (2022b). The resilience to mechanical forces provides the pathogen with a means to withstand high levels of mechanical stress during biofilm formation, thus yielding these pathogens highly resistant to breaking these cell adhesion bonds. These unusual stress-dependent molecular interactions play an integral role during bacterial colonization and dissemination and when studied, reveal critical information about pathosis Dufrêne and Viljoen (2020).

Among *S. aureus* adhesins, the bone sialoprotein binding protein (Bbp) is a bifunctional Microbial Surface Component Recognizing Adhesive Matrix Molecule (MSCRAMM) Gillaspy et al. (1998). Bbp is part of the MSCRAMM serine-aspartate repeat (Sdr) family that also includes SdrF and SdrG in *S. epidermidis*, and clumping factor A (ClfA), B (ClfB), SdrC, and SdrE in *S. aureus* Josefsson et al. (1998); McDevitt et al. (1994); Ní Eidhin et al. (1998); Tung et al. (2000). Ligand-binding for Bbp occurs generally in the N-terminal region, from residues 273 to 598, where Bbp binds to fibrinogen-α (Fgα), a glycopeptide on bone and dentine extracellular matrix (ECM). Bbp's binding region is subdivided into domains N2 and N3, which are made up of two layers of β-sheets with an open groove at the C-terminus where primary ligand binding occurs Zhang et al. (2015) (Figure 1B). The binding of Fgα follows a "dock, lock, and latch" mechanism O'Connell (2003); Ponnuraj et al. (2003); Bowden et al. (2008); Foster et al. (2014); Zhang et al. (2017), that has been previously investigated by a myriad of techniques Herman et al. (2014); Vanzieleghem et al. (2015); Vitry et al. (2017); Herman-Bausier et al. (2018); Milles et al. (2018). Thus, the pathogenic bacteria does not invade a host cell, but rather adheres to the ECM via Bbp:Fgα interactions Patti et al. (1994).

Using a combination of *in silico* and *in vitro* single-molecule force spectroscopy (SMFS), we have previously reported that *S. epidermidis*' adhesin SdrG, when in complex with Fgβ , was able to withstand extreme mechanical loads Milles et al. (2018). The necessary force applied to rupture the SdrG:Fgβ complex was shown to be an order of magnitude stronger than that needed to rupture the widely employed Streptavidin:biotin complex Sedlak et al. (2018), and more than twice of that of cellulosomal cohesin:dockerin interactions Schoeler et al. (2014); Bernardi et al. (2019). Most biological complexes rupture at a relatively low force range Seppälä et al. (2017); Haataja et al. (2019); Hoelz et al. (2011, 2012); Mendes et al. (2012); Bernardi and Pascutti (2012), including other host-pathogen interactions Bauer et al. (2022). A molecular mechanism for a catch-bond behavior of the SdrG:Fgβ was then revealed by investigating the system in a "force-clamp" regime Melo et al. (2022), with magnetic tweezers based SMFS revealing that the SdrG:Fgβ bond can live for hours under force loads Huang et al. (2022). Here, taking advantage of a powerful *in silico* SMFS approach, we describe how Bbp plays a key role in bacterial adhesion during nosocomial infections, by investigating the Bbp:Fgα complex at different pulling velocities combining all-atom (aa) and coarse-grained (CG) steered molecular dynamics (SMD) simulations (Figure 1A,B). Building on *in vitro* SMFS data, our results point to Bbp's interaction with the extracellular matrix fibrinopeptide as the most mechanostable so far investigated, independent of the loading rate. Our findings reveal that a few key interactions are responsible for the outstanding force resilience of the complex. Furthermore, our results offer insights into the development of anti-adhesion strategies.

2 RESULTS

2.1 Bbp is highly mechanostable under stress

To probe the mechanics of the interaction between Bbp and Fgα , and to characterize the atomic details of the complex under force load, we performed aa-SMD simulations with Bbp anchored by its C-terminal while Fgα was pulled at different velocities (Table S1). The simulations resulted in Force vs. extension curves that reveal a clear one-step rupture event, as represented in Figure 2A. For the slowest pulling velocity, 160 replicas were performed following a wide-sampling paradigm previously developed in our group Sedlak et al. (2020). At the pulling velocity of 2.5×10^{-04} nm/ps, we observed that the most probable rupture force for the complex was 3,510 pN, as described by the Bell-Evans (BE) Bell (1978); Evans and Ritchie (1997) fit of the peak forces at that pulling speed (see Figure 2B). Our results reveal that Bbp:Fgα is the most mechanostable complex investigated thus far, which is in agreement with previous experimental data where we showed that SdrG:Fgβ complex can withstand forces on the 2nN range, equivalent to breaking of covalent bonds Milles et al. (2018).

To investigate the dependence of the mechanostability of Bbp:Fgα on the force loading rate, we performed CG-SMD simulations at several, much lower, pulling speeds (Table S1). We have recently shown that aa-SMD and CG-SMD can be combined to in an *in silico* SMFS approach Gomes et al. (2022a); Melo et al. (2022). Here, the combination of the two levels of molecular details is capable of rendering predictions that are consistent with theory and experimentation with the advantage of being 10 to approximately 100 times faster than aa-SMD simulations, depending on the pulling speed Gomes et al. (2022a); Melo et al. (2022). A Dudko-Hummer-Szabo Dudko et al. (2006) (DHS) fit was performed through the SMD data, including both the aa-SMD, and the CG-SMD (see Figure 3). The DHS fit suggests that the system should rupture at forces higher than 2 nN at 10^5 pN/s force loading rate, in agreement with experimental data Milles et al. (2018). It is interesting to note that the BE model is able to fit well all the simulation results, at both aa and CG level, as evidenced by the density plots in Figure 3.

The influence of the peptide size on the rupture force was also investigated. We have shown previously that SdrG complexed with shortened Fgβ peptides had lower unbinding forces Milles et al. (2018). Here, we simulated a model of Bbp complexed with Fgα elongated by nine residues (See Methods section) by aa and CG-SMD simulations (Table S1). Our results show that the force loading rate was not significantly impacted by the size of the peptide (Figure S1), indicating that the original complex formed at the crystal structure has the minimal length to keep the important contacts with the protein latch to hold the DLL configuration.

2.2 Key hydrogen bonds are responsible for Bbp:Fgα high mechanostability

After confirming that Bbp:Fgα complex presents a hyperstable interaction under shear mechanical load, we used the approximately 3 μs of aa-SMD simulation data to investigate the molecular origin of the mechanostability of the complex. Previously, simulations of the SdrG:Fgβ revealed the presence of frequent and persistent hydrogen bonds (H-bonds) between the peptide and the protein backbone, showing that the high-force resilience of the complex was largely independent of the peptide side-chains interactions, and therefore the peptide's sequence Milles et al. (2018). Here, we computed the occupancy of the H-bonds between the Bbp and Fgα before the complex rupture. We identified the key amino acid interactions responsible for keeping the complex together at high force loads (Table 1). Different than SdrG:Fgβ , Bbp:Fgα interactions are not dominated by backbone-backbone interactions, with a significant amount of side-chain interaction of the peptide playing an important role in the complex mechanostability. The

backbone interactions between Bbp $^{\text{Leu584, Thr582, Thr586}}$ and Fgα $^{\text{Thr565,Ser567,Thr586}}$ have been previously described as important for Fgα binding at the crystal structure Zhang et al. (2015). However, we noticed that the side-chain H-bonds are rearranged upon application of mechanical stress on the complex. On the crystal, Bbp$^{\text{Asp334}}$ forms a side-chain H-bond with Fgα $^{\text{Ser566}}$, and during the SMD simulations, this interaction shifts to Fgα $^{\text{Thr565}}$, being the H-bond with the highest occupancy over the trajectories. Another shift occurs between Bbp$^{\text{Asp334,Ile335}}$ interacting with Fgα $^{\text{Phe564}}$, on the crystal, to Bbp$^{\text{Ser333}}$ interacting with Fgα $^{\text{Phe564}}$ in our simulations. The H-bond between Bbp$^{\text{Asp588}}$ and Fgα $^{\text{Gln563}}$ is described as important to lock the peptide N-terminus and is still present before the rupture of the complex, although with lower occupancy. Instead, a charged side-chain interaction arises with significant occupancy values: Bbp$^{\text{Asp556}}$:Fgα $^{\text{Lys562}}$. These data corroborates the importance of backbone interactions to maintain the high mechanostability and also highlights important side chain H-bonds plasticity that occurs when Bbp:Fgα is exposed to mechanical stress.

Table 1. Hydrogen bonds occupancy between Bbp and Fgα residues calculated and averaged before the main rupture event.

Bbp	Fgα	Occupancy (%)	Nature
Asp334	Thr565	54.84	Side-chain
Asp556	Lys562	45.39	Salt-bridge
Leu584	Thr565	36.14	Backbone
Thr582	Ser567	35.62	Backbone
Thr586	Gln563	35.03	Backbone:Side-chain
Ser333	Phe564	18.54	Side-chain
Asp588	Gln563	12.77	Side-chain
Thr587	Ser561	12.66	Side-chain

2.3 The force propagates indirectly from the latch to the peptide

How a shear force load "activates" the hyperstability of the complex can be investigated by analysing the evolution of pairwise interactions during the force-loading event. Such analysis can be used to investigate how a catch-bond may be formed in the Bbp:Fgα complex Liu et al. (2020). Previously, it has been shown that SdrG:Fgβ presents a catch-bond behavior Huang et al. (2022), which is expected also for Bbp:Fgα . To analyse the pairwise interactions during the SMD, we employed the generalized correlation-based dynamical network analysis method Melo et al. (2020), which can also be used to calculate force propagation pathways Schoeler et al. (2015). Figure 4A shows the pairwise interactions obtained from the network analysis. The thickness of the connections between nodes (amino acid residues) represents how well correlated the motion of these nodes are, and therefore how well connected are these amino acid residues.

The force propagation pathway that connects the pulling and the anchoring residues shows that most of the force is propagating from the protein latch directly to the peptide, passing by the center of Bbp's N2 domain (Figure 4B). These results are slightly different than the ones obtained for the SdrG:Fgβ complex upon high mechanical stress Milles et al. (2018). However, in a previous study, it was observed that changes in the pulling velocities can lead to different force propagation pathways, suggesting different unbinding mechanisms at different pulling rates Melo et al. (2022).

The rigidity of the protein under high-force load can also be studied using the betweenness map from the dynamical network analysis (see Figure 4C). The betweenness is defined as the number of shortest paths from all vertices to all others that pass through that node, in this case, an amino acid residue.

If an amino acid residue has high betweenness, it tends to be important for controlling inter-domain communication within a protein Melo et al. (2020). High betweenness values (thicker red tubes) are seen on the latch that is in direct contact with Fgα , highlighting the strong correlation between the motif and the peptide. Interestingly, high betweenness is also found at connections intra N2 domain, pointing that Bbp:Fgα complex becomes more rigid under high force loads, particularly in the region interconnecting the latch, the peptide and the N2 domains. Such behavior helps the stabilization of the interactions under high forces.

A representation of the network in subgroups, or communities, is shown at Figure 4D. The communities group the amino acid residues that are most inter-connected in relation to the rest of the network. We can see that Bbp:Fgα is subdivided in a handful of communities. The latch, most of Fgα , and part of the N2 domains are united in the same community in light blue, showing that these amino acids are highly connected. We also measured the correlation between motions on the interface residues to determine how cooperative their motion is and the essential contacts that are keeping the complex stable under high mechanical load. Essentially, the higher the correlation between residues, the more relevant is their interaction for the stability of the protein complex. We noticed that two Fgα residues are highly correlated (values equal or superior to 0.5) to Bbp at the interface, namely: Fgα $^{\text{Gln563}}$: Bbp$^{\text{Asp588,Ser585,Thr586,Thr587}}$ and Fgα $^{\text{Phe564}}$:Bbp$^{\text{Ser585}}$ (Figure 5). The importance of Fgα $^{\text{Gln563}}$ described as a persistent H-bond contact with Bbp$^{\text{Asp588,Thr586}}$ and important locking contact is reinforced by its high correlation values. The same analysis was performed for the simulations of Bbp complexed with the elongated Fgα peptide (Figure S2). The pattern of contacts is very similar, reinforcing the importance of Fgα $^{\text{Gln563}}$, and we observe the absence of new contacts made by the extra residues, corroborating that the short peptide contains the key residues responsible for holding the complex tight at the DLL configuration.

3 DISCUSSION

During infection, Gram-positive bacteria are frequently exposed to high mechanical stress. These bacteria have evolved an intricate host-binding mechanism to efficiently form colonies under the most inhospitable conditions. Key for the maintenance of the colonies, biofilms are an important virulence factor developed by *S. aureus* among other bacteria. In the initial steps of infection and biofilm formation, MSCRAMMS adhesins have an important role in clinging the bacteria to their human hosts Otto (2009); Latasa et al. (2006). *S. aureus* isolated from patients suffering from septic arthritis and osteomyelitis specifically interacts with bone sialoprotein, present at bone and dentine extracellular matrix. This interaction is mediated by an specific adhesin protein, namely Bbp Ryden et al. (1987); Ganss et al. (1999); Tung et al. (2000).

Here we have explored the interaction of Bbp with Fgα by using an *in silico* SMFS approach that relies on aa- and CG-SMD simulations. CG-SMD simulations have proven to bridge the force-loading gap between *in vitro* SMFS data with *in silico* data obtained from aa-SMD simulations, distanced by orders of magnitude Gomes et al. (2022a). In addition, CG-SMD simulations require much less computational power Liu et al. (2021); Poma et al. (2019), enabling us to explore pulling speeds unfeasible to simulate via aa-SMD Gomes et al. (2022a). Using an approach previously described Souza et al. (2019), we combined GōMartini approach Poma et al. (2017) with Martini 3 Souza et al. (2021) obtaining sensible results. The higher spread of rupture force at faster pulling rates suggests that force-induced extensions may result in lost of relevant interactions between CG-bead pairs, indicating that further optimization of the contact map or redefinition of the native contacts is necessary to improve the results Mahmood et al. (2021).

Here, we showed that Bbp:Fgα complex can withstand forces even higher than the previously investigated SdrG:Fgβ complex Milles et al. (2018) , overcoming the 2 nN force range for rupture forces, equivalent to breaking covalent bonds, demonstrating the high mechanostability of the Bbp:Fgα complex. We revealed that the force propagation pathway between the anchoring and pulling points of the Bbp:Fgα complex goes beyond the interactions between the latch and the peptide, passing through an intricate network involving several amino acids of the Bbp N2 domain (Figure 4). We were also able to point the key residues H-bonds responsible for keeping the complex stable at such high mechanical stress, highlighting important backbone-backbone interactions between Bbp$^{\text{Leu584, Thr582, Thr586}}$ and Fgα $^{\text{Thr565, Ser567,Thr586}}$ but also side-chain connections, such as Bbp$^{\text{Asp334}}$:Fgα $^{\text{Thr565}}$, Bbp$^{\text{Ser333}}$:Fgα $^{\text{Phe564}}$ and Bbp$^{\text{Asp588}}$:Fgα $^{\text{Gln563}}$ (Table 1). The latter being an important contact to lock the peptide N-terminus Zhang et al. (2015). Fgα $^{\text{Gln563}}$ has also revealed to be a key network hub, being highly correlated with several residues on the complex interface such as Bbp$^{\text{Asp588,Ser585,Thr586,Thr587}}$ (Figure 5). We also showed that the short Fgα peptide is able to hold the key interactions responsible for its mechanostability by probing an elongated Fgα in complex with Bbp (Figures S1 and S2).

By probing the Bbp:Fgα complex under high mechanical load, we discovered the molecular mechanism that triggers Bbp's unique resilience to shear forces. The high force-loads that can be found during initial stages of bacterial infection stabilize the interconnection between the protein's amino acids, particularly along the β-sheets that, due to their force-loading geometry, cannot be "peeled" like other β-sheet-rich proteins, such as green fluorescent protein (GFP) Hughes and Dougan (2016); Dietz et al. (2006) and human filamins Seppälä et al. (2017); Haataja et al. (2019). Our results build on previous knowledge of host-microbial interactions, supporting the idea that anti-adhesion therapies might be fundamental in our fight against nosocomial bacteria infections.

Antiadhesion therapies are attractive since they would not target essential processes and have the potential advantage of eliciting less and slower resistance aquisition. Some of the approaches using peptides have been reviewed elsewhere Dufrêne and Viljoen (2020). Our findings support that a short peptide is capable of holding the essential interactions to keep the protein locked in the DLL configuration. This could be explored on the design of small peptidomimetic compounds that can mimic these interactions. Moreover, peptidomimetics overcome the poor pharmacokinetic profile and low selectivity associated with peptide therapies, the main drawback for this kind of approach Li Petri et al. (2022). Another possible strategy would be to replace the peptide backbone for a small drug-like molecule with substituents that could mimic the bioactive conformation of the native peptide Spiegel et al. (2012).

Due to the good agreement between our *in-silico* SMFS protocol and experiments, we could use our simulations as a platform to study structure-activity relationships and not only screen the early potential drug candidates, but also decipher their mechanisms of action. The best candidates can be later probed by SMFS experiments. In summary, our work presents a key step in creating a intelligent design for a new class of antibiotics that act on the initial stages of bacterial infection.

4 METHODS

4.1 Structure preparation

The structure of Bbp in complex with Fgα has been previously solved by means of X-ray crystallography at 1.45 Å resolution Zhang et al. (2015) and deposited at the Protein Data Bank (PDB ID: 5CFA). Here we

retrieved this structure and prepared it for molecular dynamics (MD) simulations using VMD Humphrey et al. (1996) and its plugin QwikMD Ribeiro et al. (2016). To investigate the loading rate dependency on the size of the peptide, we used Modeller v.10.1 Webb and Sali (2016) to create an additional structure of the complex where the Fgα was elongated by 9 residues at its C-terminal end, in respect of the crystal structure, following the sequence of Fgα from *Homo sapiens* (Uniprot ID: P02671). The model followed the same preparation as described for the crystal structure.

4.2 All-atom molecular dynamics simulations

The complexes between BBP and Fgα in its short or longer configuration were solvated using the TIP3P water model Jorgensen et al. (1983), with the net charge of the protein neutralized using a 150 mM concentration of sodium chloride. Steered molecular dynamics (SMD) simulations were carried out using NAMD 3 Phillips et al. (2020), with the CHARMM36 force field Best et al. (2012). The simulations were performed assuming periodic boundary conditions in the isothermal-isobaric ensemble (NPT) with temperature maintained at 300 K using Langevin dynamics for temperature and pressure coupling, the latter kept at 1 bar. A distance cut-off of 11.0 Å was applied to short-range non-bonded interactions, whereas long-range electrostatic interactions were treated using the particle-mesh Ewald (PME) Darden et al. (1993) method. Taking advantage of a hydrogen-mass repartitioning method implemented in VMD's autopsfgen, the time step of integration was chosen to be 4 fs for all production aa-MD simulations performed. Before the SMD simulations, the system was submitted to an energy minimization protocol for 1,000 steps. An MD simulation with position restraints in the protein backbone atoms was performed for 1 ns, with temperature ramping from 0 K to 300 K in the first 0.5 ns at a timestep of 2.0 fs in the NVT ensemble, which served to pre-equilibrate the system. In an *in silico* single molecule force spectroscopy (SMFS) strategy Verdorfer et al. (2017); Bernardi et al. (2019), SMD simulations were carried out in several replicas, using a constant velocity stretching protocol at three different pulling speeds (Table S1). SMD was employed by harmonically restraining the position of the amino acid at the C-ter of Bbp and moving a second restraint point at the C-ter of Fgα peptide with a 5 kcal/mol Å^2 spring constant, with constant velocity in the z axis. The force applied to the harmonic spring is then monitored during the time of the SMD. The pulling point was moved with constant velocity along the z-axis and due to the single anchoring point and the single pulling point the system is quickly aligned along the z-axis. The number of replicas for each velocity is indicated at Table S1.

4.3 Coarse-grained molecular dynamics simulations

The atomistic model of Bbp:Fgα was modeled onto the Martini 3.0 Coarse-grained (CG) force field (v.3.0.b.3.2) Souza et al. (2021) using martinize2 v0.7.3 Kroon (2020). A set of native contacts, based on the rCSU+OV contact map protocol, was computed from the equilibrated all-atom structure using the rCSU server Wołek et al. (2015) and used to determine Gö-MARTINI interactions Poma et al. (2017) used to restraint the secondary and tertiary structures with the effective depth ϵ of Lennard-Jones potential set to 9.414 kJ.mol^{-1}. All CG-MD simulations were performed using GROMACS version 2021.5 Abraham et al. (2015). The Bbp:Fgα complex was centered in a rectangular box measuring with 10.0, 10.0, 25.0 nm to the x,y, and z directions. The anchor (Bbp C-terminal) and pulling (peptide C-terminal) backbone (BB) atoms were used to align the protein to the Z axis. The box was then solvated with Martini3 water molecules. Systems were minimized for 10,000 steps with steepest descent, followed by a 10 ns equilibration at the NPT ensemble using the Berendsen thermostat at 298K, while pressure was kept at 1 bar with compressibility set to 3e^{-4}bar^{-1}, using the Berendsen barostat. A time step of 10 fs was used to integrate the equations of motion. Pulling simulations were subsequently done at the NVT ensemble with a

time step of 20 fs. The temperature was controlled using the v-rescale thermostat Bussi et al. (2007) with a coupling time of 1 ps. For all CG-MD simulations, the cutoff distance for Coulombic and Lennard-Jones interactions was set to 1.1 nm De Jong et al. (2016), with the long-range Coulomb interactions treated by a reaction field (RF) Tironi et al. (1995) with ϵ_r=15. The Verlet neighbor search Verlet (1967) was used in combination with the neighbor list, updated every 20 steps. The LINCS Hess et al. (1997) algorithm was used to constrain the bonds and the leapfrog integration algorithm for the solution of the equations of motion. Several replicas of CG-SMD simulations were performed at a range of speeds described at Table S1.

4.4 Simulation data analysis

All analysis presented at the main text correspond to the Bbp:Fgα original complex. Force loading rate and mean correlation values for Bbp complexed with the elongated Fgα peptide are found on the Supplementary Information material. H-bonds occupancy between Bbp and Fgα were calculated and averaged for aa-MD simulations 1 ns before the main rupture event, using VMD Humphrey et al. (1996) with standard parameters for the calculation: residue pairs; donor-acceptor distance of 3.0 Å; angle cutoff of 20 degrees. Mean correlation and dynamical network pathways were calculated using the generalized dynamical network analysis Melo et al. (2020) and VMD for aa-SMD at pulling velocity of 2.5×10^{-4} nm/ps. In this analysis, a network is defined as a set of nodes that represent amino acid residues, and the node's position is mapped to that of the residue's α-carbon. Edges connect pairs of nodes if their corresponding residues are in contact, and 2 non-consecutive residues are said to be in contact if they are within 4.5 Å of each other for at least 75% of analyzed frames. The interface residues between Bbp:Fgα were defined in a radius of 10 Å between nodes in each molecule. A representative for the full-network, optimal and suboptimal paths and communities was rendered using one of the SMD trajectory replicas. The mean correlation analysis was carried out 1ns before the first rupture event using a cutoff of 0.35 for the mean correlation coefficients. All charts were generated using in-house python scripts. The protein image was rendered using VMD.

CONFLICT OF INTEREST STATEMENT

The authors declare that the research was conducted in the absence of any commercial or financial relationships that could be construed as a potential conflict of interest.

AUTHOR CONTRIBUTIONS

PSFCG, MF and MP contributed to performing simulations, analysing data, and writing of the manuscript. DG contributed to analysing data and discussion. RB contributed to writing and discussion on *in silico* force spectroscopy, proof-reading, manuscript revision and approval of the submitted version. PSFCG and RB coordinated the project.

FUNDING

This work was supported by the National Science Foundation under Grant MCB-2143787 (CAREER: *In Silico* Single-Molecule Force Spectroscopy) and ACCESS Allocations (Project: BIO220009). We thank Auburn University and the College of Sciences and Mathematics for the computational resources provided by Dr. Bernardi faculty startup funds.

ACKNOWLEDGMENTS

We thank Dr. Marcelo Melo for the fruitful discussions.

DATA AVAILABILITY STATEMENT

The datasets for this study can be available upon reasonable request to the corresponding author.

REFERENCES

Abraham, M. J., Murtola, T., Schulz, R., Páll, S., Smith, J. C., Hess, B., et al. (2015). Gromacs: High performance molecular simulations through multi-level parallelism from laptops to supercomputers. *SoftwareX* 1-2, 19–25. doi:10.1016/j.softx.2015.06.001

Archer, N. K., Mazaitis, M. J., Costerton, J. W., Leid, J. G., Powers, M. E., and Shirtliff, M. E. (2011). Staphylococcus aureus biofilms: properties, regulation, and roles in human disease. *Virulence* 2, 445–459

Bai, A. D., Lo, C. K., Komorowski, A. S., Suresh, M., Guo, K., Garg, A., et al. (2022). Staphylococcus aureus bacteremia mortality: a systematic review and meta-analysis. *Clinical Microbiology and Infection*

Bauer, M. S., Gruber, S., Hausch, A., Gomes, P. S., Milles, L. F., Nicolaus, T., et al. (2022). A tethered ligand assay to probe SARS-CoV-2:ACE2 interactions. *Proceedings of the National Academy of Sciences* 119, e2114397119

Bell, G. I. (1978). Models for the specific adhesion of cells to cells. *Science* 200, 618–627

Bernardi, R. C., Durner, E., Schoeler, C., Malinowska, K. H., Carvalho, B. G., Bayer, E. A., et al. (2019). Mechanisms of nanonewton mechanostability in a protein complex revealed by molecular dynamics simulations and single-molecule force spectroscopy. *Journal of the American Chemical Society* 141, 14752–14763

Bernardi, R. C. and Pascutti, P. G. (2012). Hybrid qm/mm molecular dynamics study of benzocaine in a membrane environment: How does a quantum mechanical treatment of both anesthetic and lipids affect their interaction. *Journal of chemical theory and computation* 8, 2197–2203

Best, R. B., Zhu, X., Shim, J., Lopes, P. E., Mittal, J., Feig, M., et al. (2012). Optimization of the additive charmm all-atom protein force field targeting improved sampling of the backbone ϕ, ψ and side-chain $\chi1$ and $\chi2$ dihedral angles. *Journal of chemical theory and computation* 8, 3257–3273

Bowden, M. G., Heuck, A. P., Ponnuraj, K., Kolosova, E., Choe, D., Gurusiddappa, S., et al. (2008). Evidence for the "dock, lock, and latch" ligand binding mechanism of the staphylococcal microbial surface component recognizing adhesive matrix molecules (mscramm) sdrg. *Journal of Biological Chemistry* 283, 638–647

Bussi, G., Donadio, D., and Parrinello, M. (2007). Canonical sampling through velocity rescaling. *The Journal of chemical physics* 126, 014101

Costerton, J. W., Stewart, P. S., and Greenberg, E. P. (1999). Bacterial biofilms: a common cause of persistent infections. *Science* 284, 1318–1322

Darden, T., York, D., and Pedersen, L. (1993). Particle mesh ewald: An n log (n) method for ewald sums in large systems. *The Journal of chemical physics* 98, 10089–10092

De Jong, D. H., Baoukina, S., Ingólfsson, H. I., and Marrink, S. J. (2016). Martini straight: Boosting performance using a shorter cutoff and gpus. *Computer Physics Communications* 199, 1–7

Dietz, H., Berkemeier, F., Bertz, M., and Rief, M. (2006). Anisotropic deformation response of single protein molecules. *Proceedings of the National Academy of Sciences* 103, 12724–12728

Donkor, E. S. and Kotey, F. C. (2020). Methicillin-resistant staphylococcus aureus in the oral cavity: Implications for antibiotic prophylaxis and surveillance. *Infectious Diseases: Research and Treatment* 13, 1178633720976581

Dudko, O. K., Hummer, G., and Szabo, A. (2006). Intrinsic rates and activation free energies from single-molecule pulling experiments. *Phys. Rev. Lett.* 96, 108101. doi:10.1103/PhysRevLett.96.108101

Dufrêne, Y. F. and Viljoen, A. (2020). Binding strength of gram-positive bacterial adhesins. *Frontiers in microbiology* 11, 1457

Evans, E. and Ritchie, K. (1997). Dynamic strength of molecular adhesion bonds. *Biophysical journal* 72, 1541–1555

Foster, T. J., Geoghegan, J. A., Ganesh, V. K., and Höök, M. (2014). Adhesion, invasion and evasion: the many functions of the surface proteins of staphylococcus aureus. *Nature reviews microbiology* 12, 49–62

Ganss, B., Kim, R. H., and Sodek, J. (1999). Bone sialoprotein. *Critical Reviews in Oral Biology & Medicine* 10, 79–98

Garbacz, K., Kwapisz, E., Piechowicz, L., and Wierzbowska, M. (2021). Staphylococcus aureus isolated from the oral cavity: Phage susceptibility in relation to antibiotic resistance. *Antibiotics* 10, 1329

Gillaspy, A. F., Lee, C. Y., Sau, S., Cheung, A. L., and Smeltzer, M. S. (1998). Factors affecting the collagen binding capacity of staphylococcus aureus. *Infection and immunity* 66, 3170–3178

Gomes, D. E., Melo, M. C., Gomes, P. S., and Bernardi, R. C. (2022a). Bridging the gab between in vitro and in silico single-molecule force spectroscopy. *bioRxiv*

Gomes, P. S. F. C., Gomes, D. E. B., and Bernardi, R. C. (2022b). Protein structure prediction in the era of ai: Challenges and limitations when applying to in silico force spectroscopy. *Frontiers in Bioinformatics* 2, 983306. doi:10.3389/fbinf.2022.983306

González, J. F., Hahn, M. M., and Gunn, J. S. (2018). Chronic biofilm-based infections: skewing of the immune response. *Pathogens and disease* 76, fty023

Haataja, T. J., Bernardi, R. C., Lecointe, S., Capoulade, R., Merot, J., and Pentikäinen, U. (2019). Non-syndromic mitral valve dysplasia mutation changes the force resilience and interaction of human filamin a. *Structure* 27, 102–112

Herman, P., El-Kirat-Chatel, S., Beaussart, A., Geoghegan, J. A., Foster, T. J., and Dufrêne, Y. F. (2014). The binding force of the staphylococcal adhesin sdrg is remarkably strong. *Molecular microbiology* 93, 356–368

Herman-Bausier, P., Labate, C., Towell, A. M., Derclaye, S., Geoghegan, J. A., and Dufrêne, Y. F. (2018). Staphylococcus aureus clumping factor a is a force-sensitive molecular switch that activates bacterial adhesion. *Proceedings of the National Academy of Sciences* 115, 5564–5569

Hess, B., Bekker, H., Berendsen, H. J., and Fraaije, J. G. (1997). Lincs: a linear constraint solver for molecular simulations. *Journal of computational chemistry* 18, 1463–1472

Hoelz, L. V., Bernardi, R. C., Horta, B. A., Araújo, J. Q., Albuquerque, M. G., da Silva, J. F., et al. (2011). Dynamical behaviour of the human β1-adrenoceptor under agonist binding. *Molecular Simulation* 37, 907–913

Hoelz, L. V., Ribeiro, A. A., Bernardi, R. C., Horta, B. A., Albuquerque, M. G., da Silva, J. F., et al. (2012). The role of helices 5 and 6 on the human β1-adrenoceptor activation mechanism. *Molecular Simulation* 38, 236–240

Huang, W., Le, S., Sun, Y., Lin, D. J., Yao, M., Shi, Y., et al. (2022). Mechanical stabilization of a bacterial adhesion complex. *Journal of the American Chemical Society* 144, 16808–16818

Hughes, M. L. and Dougan, L. (2016). The physics of pulling polyproteins: a review of single molecule force spectroscopy using the afm to study protein unfolding. *Reports on Progress in Physics* 79, 076601

Humphrey, W., Dalke, A., and Schulten, K. (1996). Vmd: visual molecular dynamics. *Journal of molecular graphics* 14, 33–38

Jevon, P., Abdelrahman, A., and Pigadas, N. (2021). Management of odontogenic infections and sepsis: an update. *Bdj Team* 8, 24–31

Jorgensen, W. L., Chandrasekhar, J., Madura, J. D., Impey, R. W., and Klein, M. L. (1983). Comparison of simple potential functions for simulating liquid water. *The Journal of chemical physics* 79, 926–935

Josefsson, E., McCrea, K. W., Eidhin, D. N., O'Connell, D., Cox, J., Hook, M., et al. (1998). Three new members of the serine-aspartate repeat protein multigene family of staphylococcus aureus. *Microbiology* 144, 3387–3395

Kroon, P. (2020). *Aggregate, automate, assemble*. Ph.D. thesis, University of Groningen

Kwiecinski, J. M. and Horswill, A. R. (2020). Staphylococcus aureus bloodstream infections: pathogenesis and regulatory mechanisms. *Current opinion in microbiology* 53, 51–60

Latasa, C., Solano, C., Penadés, J. R., and Lasa, I. (2006). Biofilm-associated proteins. *Comptes rendus biologies* 329, 849–857

Li Petri, G., Di Martino, S., and De Rosa, M. (2022). Peptidomimetics: An overview of recent medicinal chemistry efforts toward the discovery of novel small molecule inhibitors. *Journal of Medicinal Chemistry*

Lister, J. L. and Horswill, A. R. (2014). Staphylococcus aureus biofilms: recent developments in biofilm dispersal. *Frontiers in cellular and infection microbiology* 4, 178

Liu, Z., Liu, H., Vera, A. M., Bernardi, R. C., Tinnefeld, P., and Nash, M. A. (2020). High force catch bond mechanism of bacterial adhesion in the human gut. *Nature communications* 11, 1–12

Liu, Z., Moreira, R. A., Dujmovic, A., Liu, H., Yang, B., Poma, A. B., et al. (2021). Mapping mechanostable pulling geometries of a therapeutic anticalin/ctla-4 protein complex. *Nano letters* 22, 179–187

Mahmood, M. I., Poma, A. B., and Okazaki, K.-i. (2021). Optimizing gō-martini coarse-grained model for f-bar protein on lipid membrane. *Frontiers in Molecular Biosciences* 8. doi:10.3389/fmolb.2021.619381

McCormack, M., Smith, A., Akram, A., Jackson, M., Robertson, D., and Edwards, G. (2015). Staphylococcus aureus and the oral cavity: an overlooked source of carriage and infection? *American journal of infection control* 43, 35–37

McDevitt, D., Francois, P., Vaudaux, P., and Foster, T. (1994). Molecular characterization of the clumping factor (fibrinogen receptor) of staphylococcus aureus. *Molecular microbiology* 11, 237–248

Melo, M. C., Bernardi, R. C., De La Fuente-Nunez, C., and Luthey-Schulten, Z. (2020). Generalized correlation-based dynamical network analysis: a new high-performance approach for identifying allosteric communications in molecular dynamics trajectories. *The Journal of Chemical Physics* 153, 134104

Melo, M. C., Gomes, D. E., and Bernardi, R. C. (2022). Molecular origins of force-dependent protein complex stabilization during bacterial infections. *Journal of the American Chemical Society* 145, 70–77

Mendes, Y. S., Alves, N. S., Souza, T. L., Sousa Jr, I. P., Bianconi, M. L., Bernardi, R. C., et al. (2012). The structural dynamics of the flavivirus fusion peptide–membrane interaction

Milles, L. F., Schulten, K., Gaub, H. E., and Bernardi, R. C. (2018). Molecular mechanism of extreme mechanostability in a pathogen adhesin. *Science* 359, 1527–1533

Ní Eidhin, D., Perkins, S., Francois, P., Vaudaux, P., Höök, M., and Foster, T. J. (1998). Clumping factor b (clfb), a new surface-located fibrinogen-binding adhesin of staphylococcus aureus. *Molecular microbiology* 30, 245–257

O'Connell, D. (2003). Dock, lock and latch. *Nature Reviews Microbiology* 1, 171–171

Otto, M. (2009). Staphylococcus epidermidis—the'accidental'pathogen. *Nature reviews microbiology* 7, 555–567

Patti, J. M., Allen, B. L., McGavin, M. J., and Höök, M. (1994). Mscramm-mediated adherence of microorganisms to host tissues. *Annual Reviews in Microbiology* 48, 585–617

Phillips, J. C., Hardy, D. J., Maia, J. D., Stone, J. E., Ribeiro, J. V., Bernardi, R. C., et al. (2020). Scalable molecular dynamics on cpu and gpu architectures with namd. *The Journal of chemical physics* 153, 044130

Poma, A. B., Cieplak, M., and Theodorakis, P. E. (2017). Combining the martini and structure-based coarse-grained approaches for the molecular dynamics studies of conformational transitions in proteins. *Journal of Chemical Theory and Computation* 13, 1366–1374

Poma, A. B., Guzman, H. V., Li, M. S., and Theodorakis, P. E. (2019). Mechanical and thermodynamic properties of aβ42, aβ40, and α-synuclein fibrils: a coarse-grained method to complement experimental studies. *Beilstein Journal of Nanotechnology* 10, 500–513

Ponnuraj, K., Bowden, M. G., Davis, S., Gurusiddappa, S., Moore, D., Choe, D., et al. (2003). A "dock, lock, and latch" structural model for a staphylococcal adhesin binding to fibrinogen. *Cell* 115, 217–228

Ribeiro, J. V., Bernardi, R. C., Rudack, T., Stone, J. E., Phillips, J. C., Freddolino, P. L., et al. (2016). Qwikmd—integrative molecular dynamics toolkit for novices and experts. *Scientific reports* 6, 1–14

Ryden, C., Maxe, I., Franzén, A., Ljungh, A., Heinegård, D., and Rubin, K. (1987). Selective binding of bone matrix sialoprotein to staphylococcus aureus in osteomyelitis. *The Lancet* 330, 515

Schoeler, C., Bernardi, R. C., Malinowska, K. H., Durner, E., Ott, W., Bayer, E. A., et al. (2015). Mapping mechanical force propagation through biomolecular complexes. *Nano letters* 15, 7370–7376

Schoeler, C., Malinowska, K. H., Bernardi, R. C., Milles, L. F., Jobst, M. A., Durner, E., et al. (2014). Ultrastable cellulosome-adhesion complex tightens under load. *Nature communications* 5, 1–8

Sedlak, S. M., Schendel, L. C., Gaub, H. E., and Bernardi, R. C. (2020). Streptavidin/biotin: Tethering geometry defines unbinding mechanics. *Science advances* 6, eaay5999

Sedlak, S. M., Schendel, L. C., Melo, M. C., Pippig, D. A., Luthey-Schulten, Z., Gaub, H. E., et al. (2018). Direction matters: Monovalent streptavidin/biotin complex under load. *Nano letters* 19, 3415–3421

Seppälä, J., Bernardi, R. C., Haataja, T. J., Hellman, M., Pentikäinen, O. T., Schulten, K., et al. (2017). Skeletal dysplasia mutations effect on human filamins' structure and mechanosensing. *Scientific reports* 7, 1–14

Sharma, D., Misba, L., and Khan, A. U. (2019). Antibiotics versus biofilm: an emerging battleground in microbial communities. *Antimicrobial Resistance & Infection Control* 8, 1–10

Souza, P. C., Alessandri, R., Barnoud, J., Thallmair, S., Faustino, I., Grünewald, F., et al. (2021). Martini 3: a general purpose force field for coarse-grained molecular dynamics. *Nature methods* 18, 382–388

Souza, P. C. T., Thallmair, S., Marrink, S. J., and Mera-Adasme, R. (2019). An allosteric pathway in copper, zinc superoxide dismutase unravels the molecular mechanism of the g93a amyotrophic lateral sclerosis-linked mutation. *The Journal of Physical Chemistry Letters* 10, 7740–7744. doi:10.1021/acs.jpclett.9b02868. PMID: 31747286

Spiegel, J., Mas-Moruno, C., Kessler, H., and Lubell, W. D. (2012). Cyclic aza-peptide integrin ligand synthesis and biological activity. *The Journal of organic chemistry* 77, 5271–5278

Suresh, M. K., Biswas, R., and Biswas, L. (2019). An update on recent developments in the prevention and treatment of staphylococcus aureus biofilms. *International Journal of Medical Microbiology* 309, 1–12

Tironi, I. G., Sperb, R., Smith, P. E., and van Gunsteren, W. F. (1995). A generalized reaction field method for molecular dynamics simulations. *The Journal of chemical physics* 102, 5451–5459

Tung, H.-s., GUSS, B., HELLMAN, U., PERSSON, L., RUBIN, K., and RYDÉN, C. (2000). A bone sialoprotein-binding protein from staphylococcus aureus: a member of the staphylococcal sdr family. *Biochemical Journal* 345, 611–619

Vanzieleghem, T., Herman-Bausier, P., Dufrene, Y. F., and Mahillon, J. (2015). Staphylococcus epidermidis affinity for fibrinogen-coated surfaces correlates with the abundance of the sdrg adhesin on the cell surface. *Langmuir* 31, 4713–4721

Verdorfer, T., Bernardi, R. C., Meinhold, A., Ott, W., Luthey-Schulten, Z., Nash, M. A., et al. (2017). Combining in vitro and in silico single-molecule force spectroscopy to characterize and tune cellulosomal scaffoldin mechanics. *Journal of the American Chemical Society* 139, 17841–17852

Verlet, L. (1967). Computer" experiments" on classical fluids. i. thermodynamical properties of lennard-jones molecules. *Physical review* 159, 98

Versey, Z., da Cruz Nizer, W. S., Russell, E., Zigic, S., DeZeeuw, K. G., Marek, J. E., et al. (2021). Biofilm-innate immune interface: contribution to chronic wound formation. *Frontiers in Immunology* 12, 648554

Vitry, P., Valotteau, C., Feuillie, C., Bernard, S., Alsteens, D., Geoghegan, J. A., et al. (2017). Force-induced strengthening of the interaction between staphylococcus aureus clumping factor b and loricrin. *MBio* 8, e01748–17

Webb, B. and Sali, A. (2016). Comparative protein structure modeling using modeller. *Current protocols in bioinformatics* 54, 5–6

Wertheim, H. F., Vos, M. C., Ott, A., van Belkum, A., Voss, A., Kluytmans, J. A., et al. (2004). Risk and outcome of nosocomial staphylococcus aureus bacteraemia in nasal carriers versus non-carriers. *The Lancet* 364, 703–705

Wołek, K., Gómez-Sicilia, À., and Cieplak, M. (2015). Determination of contact maps in proteins: a combination of structural and chemical approaches. *The Journal of Chemical Physics* 143, 243105

Zhang, X., Wu, M., Zhuo, W., Gu, J., Zhang, S., Ge, J., et al. (2015). Crystal structures of bbp from staphylococcus aureus reveal the ligand binding mechanism with fibrinogen α. *Protein & cell* 6, 757–766

Zhang, Y., Wu, M., Hang, T., Wang, C., Yang, Y., Pan, W., et al. (2017). Staphylococcus aureus sdre captures complement factor h's c-terminus via a novel 'close, dock, lock and latch'mechanism for complement evasion. *Biochemical Journal* 474, 1619–1631

FIGURE CAPTIONS

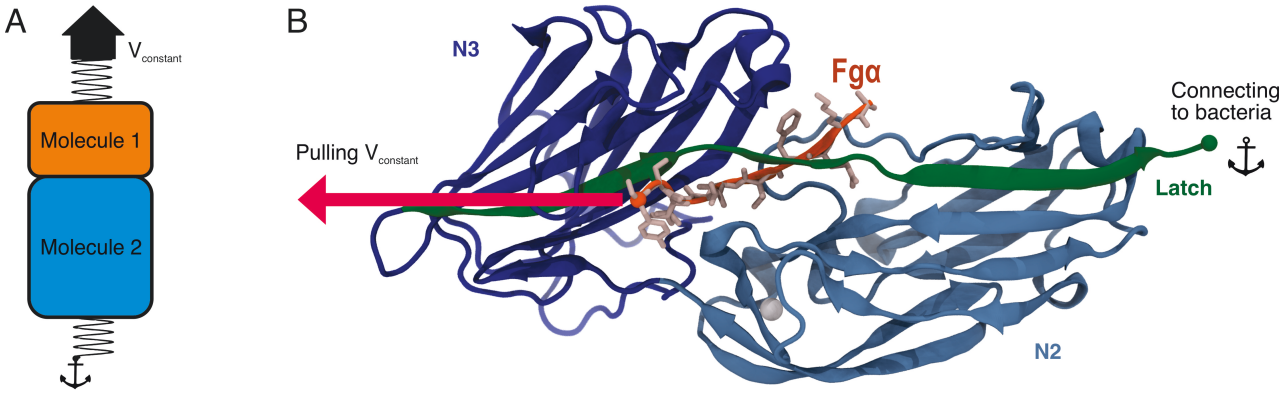

Figure 1. Bbp's adhesion domain. **a)** Scheme illustrating the SMD protocol applying force at the interface between two molecules of interest. In this protocol, a spring is attached to one of the termini of each molecule, in our case, the C-terminal end of both Bbp and Fgα peptide. While the end of Molecule 2 is fixed, the end of molecule 1 is then pulled at constant velocity. **B)** Tridimensional structure of Bbp. The protein is represented in cartoon, colored by its different domains. The latch is highlighted in green. Fgα is colored in orange and its aminoacids represented as sticks colored in light pink. The SMD pulling and anchor points are indicated in the image as spheres.

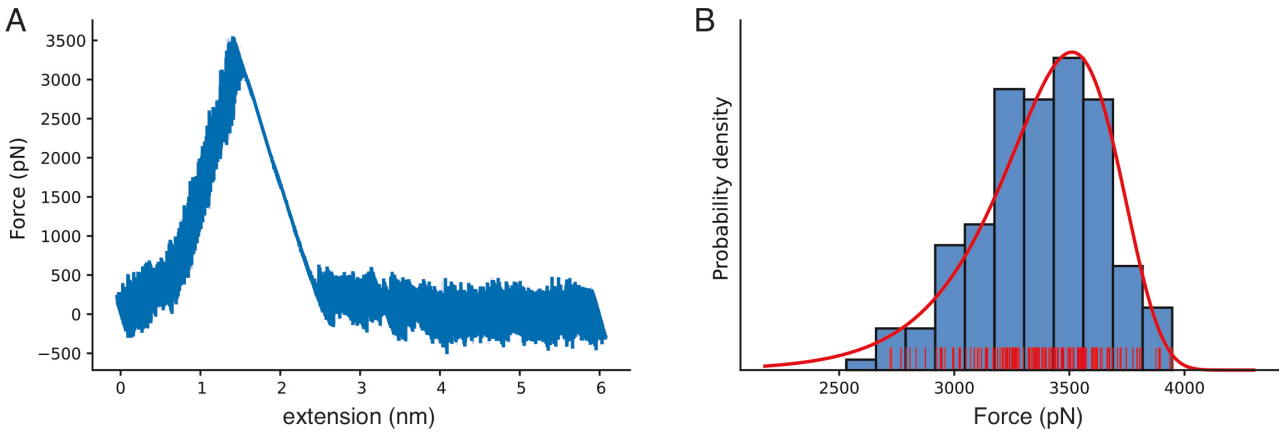

Figure 2. Bbp mechanostability under high mechanical load. **a)** Force versus extension curve as an exemplary trace, with rupture peak force at 3,510 pN. **b)** Histogram for the most probable rupture force (blue, rugged plot in red) with the Bell-Evans (BE) model for the first rupture peak (red), based on the aa-SMD simulation replicas with the slowest simulated pulling velocity (2.5×10^{-4} nm/ps).

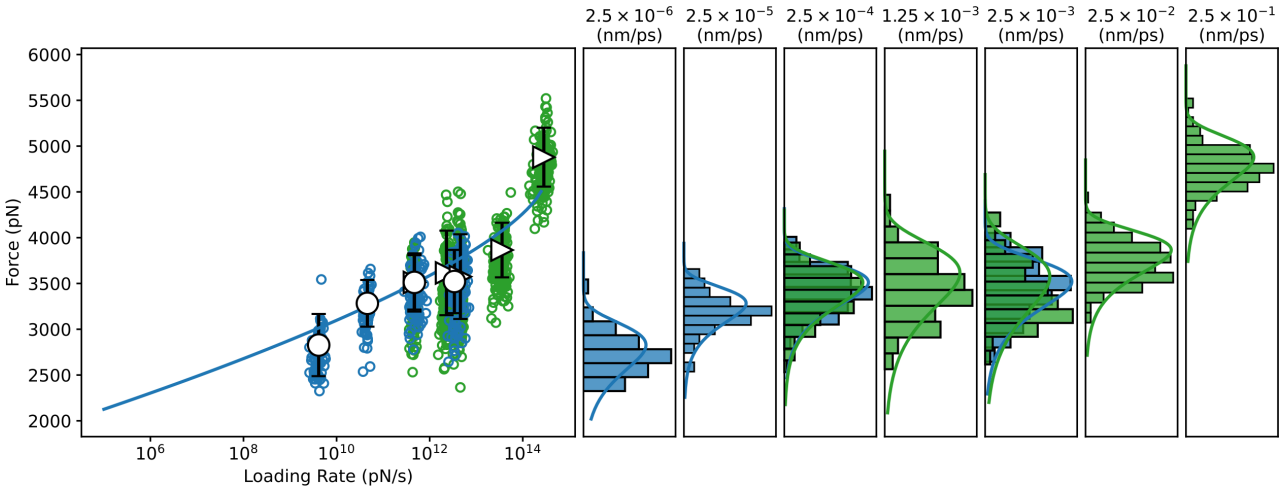

Figure 3. Dynamic Force spectrum for the Bbp:Fgα complex combining data from all-atom and coarse-grained SMD simulations. All-atom, and Coarse-grained steered molecular dynamics simulations (CG-SMD and aa-SMD) were performed at different velocities: 2.5×10^{-6} to 2.5×10^{-3} nm/ps (blue) and 2.5×10^{-4} to 2.5×10^{-3} nm/ps (green), respectively. A Dudko-Hummer-Szabo Dudko et al. (2006) (DHS) fit was performed through the SMD dataset predicting $\Delta x = 7.489 \times 10^{-2}\ nm$, $k_{off}{}^{0} = 2.596 \times 10^{-12}\ s^{-1}$, $\Delta G = 2.293 \times 10^{2}\ k_B T$.

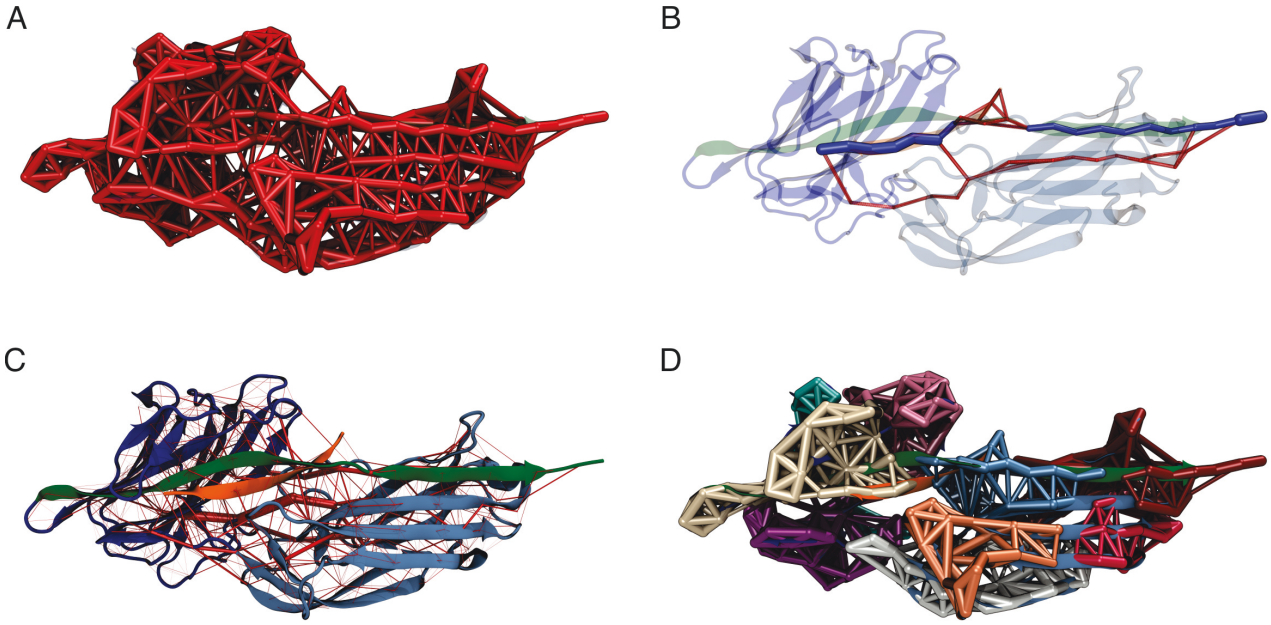

Figure 4. Bbp:Fgα dynamical network under high mechanical load. **a)** Representation of the dynamical network. The thickness of the links between the nodes (amino acid residues) represents the correlation of motion between these residues. **b)** The force propagates from the latch indirectly to the peptide, passing by the N2 domain of the protein. The color scheme of the complex is the same from Figure 1. The network's optimal path is colored in dark blue while the sub-optimal paths are colored in red. **c)** Full dynamical network revealing the most correlated regions of the complex. The weight of the network edges (represented by the thickness of red tubes) is given by the betweenness values. **d)** Generalized correlation-based communities represented by different colors of the nodes and edges in the network.

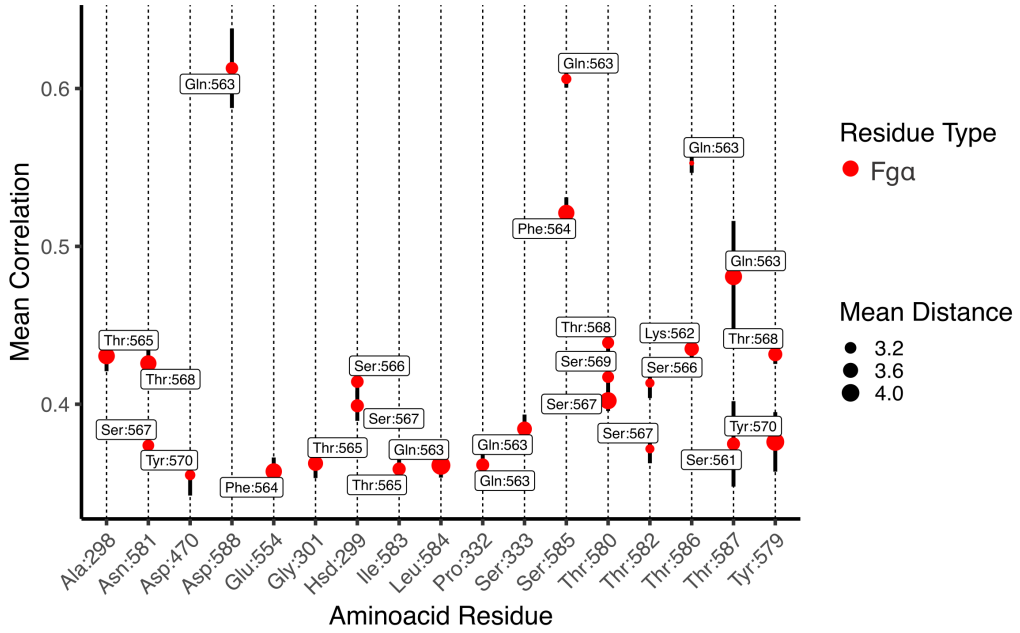

Figure 5. Mean generalized coefficients for contacts along Bbp:Fgα interface. The x axis is labeled by Bbp amino acid residues and the y axis indicates the averaged generalized correlation values (vertical bars indicate the standard error of the mean), labeled by Fgα aminoacid residues. The circle sizes indicates the average Cartesian distance. Only amino acid residues with a mean correlation higher than 0.35 are shown.